NON-PEER REVIEWED PREPRINT

Forecasting the moisture content of live forest fuels with a transformer machine learning model and Sentinel-2 satellite data

Ivan Kotzur[AB*], Matthias Boer[A], Vitus Benson[C], Rachael Nolan[AB]

[A] Hawkesbury Institute for the Environment, Western Sydney University, Richmond, NSW, Australia

[B] NSW Bushfire and Natural Hazards Research Centre, Richmond, NSW, Australia

[C] Biogeochemical Integration, Max Planck Institute for Biogeochemistry, Jena, Germany

[*]i.kotzur@westernsydney.edu.au

Abstract

Live fuel moisture content (LFMC) provides an indicator of vegetation flammability, the potential for canopy dieback from drought, and habitat quality for arboreal fauna. Recent advances in artificial intelligence have increased the potential in meteorological forecasts for Earth surface forecasting. Combining weather forecasts with remotely sensed LFMC offers a promising avenue for short and medium-term LFMC forecasting (i.e. weeks to months). We adapted a transformer-based surface forecasting model to predict LFMC across the forest regions of New South Wales, Australia, up to 50 days in advance. Using a multi-modal spatiotemporal transformer (Contextformer) as a hind-cast model of LFMC with 'minicubes' of weather, soil, vegetation structure, elevation and Sentinel-2 reflectance data, we tested four variants to evaluate if theory-guided biophysical predictors improve performance compared to the base model. Explainable AI methods were applied to demystify model reliance, using Integrated Gradients attribution. Incorporating biophysical theory in predictor selection produced the lowest error (Global RMSE=15.68% dry matter), whereas adding only spectral bands to the base model was less successful (partly due to the structure of the forecast architecture). Within the LFMC forecast, explainable AI revealed mixed patterns in importance amongst temperature and rainfall variables due to the transformer's ability to model multiple eco-physiological pathways to vegetation hydration. Dynamic weather variations dominate forecasted LFMC temporal trends, over spectral bands. Crucially, regression-to-the-mean effects in the LFMC forecasts caused poorer local performance (median R^2≈0.21) compared to global evaluation (R^2≈0.69, i.e. poorer within minicubes than amongst minicubes). When converting this hind-cast model to an operational model (i.e. true forecast), best performance could be utilised by running rolling short-term forecasts (5 to 15 days) to capture localised fuel hazard peaks and canopy dieback in the future.

Highlights

- 50-day LFMC forecasts had low Global Error (15.68% dry matter content)
- Best forecast with the additional biophysically relevant predictors
- Seasonal differences in degree of importance of temperature, the most influential driver, relative to rainfall, indicates the capture of LFMC first principles

- Regression-to-the-mean effects in the forecasts caused poorer local performance compared to global performance

1. Introduction

The frequency of extreme, high-intensity wildfires is increasing in many forest biomes, particularly the boreal and temperate forests of the northern hemisphere, but also across southern Africa, South America, and Australia (Cunningham et al. 2024). In these forest biomes, extreme fire seasons occur when fuels are in a dry state (Jain et al. 2024; Abram et al. 2021; Abatzoglou and Williams 2016). Fuel is any live or dead biomass, with fine fuels, i.e. leaves, twigs and bark less than 6 mm thick, most important for fire ignition and spread (Matthews 2013). Although the role of live fuel moisture content (LFMC) on fire behaviour is more debated than the role of dead fuel moisture content (Alexander and Cruz 2012; Rossa and Fernandes 2018), many studies have demonstrated a link between low LFMC and wildfire extent (Dennison and Moritz 2009; Argañaraz et al. 2018; Nolan et al. 2016). LFMC, calculated as the ratio of plant moisture to plant dry matter, can provide an indication of when drought is driving dieback in forest canopies, which affects the ratio of dead to live fuels and the forest microclimate (Quan et al. 2026), which in turn affect fire potential behaviour (Banerjee 2026; Ruthrof et al. 2016). Foliar moisture content, which is the same as LFMC but using different terminology, is also important for mammalian arboreal fauna, with many species relying on foliage to meet their water demands (Mella et al. 2019; Ellis et al. 1995; Kotzur 2024). Thus, the capacity to forecast LFMC is important for both seasonal fire planning and wildfire preparedness, and for responding to active fires (Burton et al. 2026), in addition to managing biodiversity.

Attempts to forecast LFMC fall into four broad categories, namely, models based on meteorological metrics, remote sensing models, mechanistic plant hydraulic models, or some combination of the above. Early efforts to model LFMC were based on drought metrics, or soil moisture, with the assumption that live fuels behaved like very wet dead fuels (Viegas et al. 2001; Qi et al. 2012; Dimitrakopoulos and Bemmerzouk 2003). However, LFMC is driven not just by weather, but also by plant physiological and morphological attributes, such as rooting depth and stomatal responses to soil and atmospheric drying (Nolan et al. 2020). Remote sensing of LFMC overcomes important limitations of models based on drought by capturing the spectral response of vegetation canopies to environmental dryness; a variety of remote sensing models have been developed that predict LFMC in near real-time (Watt et al. 2025; Yebra et al. 2013), with recent advances providing global (Quan et al. 2021), sub-daily (Quan et al. 2024) or high spatial resolution estimates (Kotzur et al. 2026). However, remote sensing alone may offer poor forecasting capability, unless combined with meteorological data. Several studies have demonstrated the potential for forecasting LFMC by correlating remotely sensed LFMC with forecastable meteorological variables. These models include regressions between the Normalised Difference Vegetation Index (NDVI) and measures such as air temperature, wind speed and drought indices (Costa-Saura et al. 2021; García et al. 2008; Chuvieco et al. 2004); remotely sensed LFMC and soil moisture (Vinodkumar et al. 2021), or some combination of these metrics (Wang and Quan 2023; Santos et al. 2026). Building on these approaches, recent advances in artificial intelligence have increased the potential within weather data for forecasting related environmental variables, when combining weather with other modes of geospatial and remote sensing data. Remote sensing of LFMC at fine spatial resolution has been successful with improvements occurring in terms of accuracy and resolution (Yebra et al. 2026; Kotzur et al. 2026). Recent advances in self-supervised forecasting of remotely sensed surface reflectance allows the extension of remote sensing measures into the future by combining approaches from video prediction and data-driven Earth system modelling (Requena-Mesa et al. June 2021). Specifically, weather forecasts are leveraged to condition a new forecast of a related land surface variable based on the past timeseries of that variable (Pellicer-Valero et al. 2025). This image-based prediction task, which was originally developed to observe the impacts of extreme weather on Earth's surface, is suitable for LFMC prediction, which is driven largely by variations in weather. Other relevant predictors can be included, in addition to the weather forecasts, as biophysical conditions in the form of either static or temporally dynamic features (Benson et al. 2024). Many biophysical variables influence plant water uptake and transpiration, and therefore LFMC, e.g. rooting patterns and leaf traits such as leaf mass per area (Griebel et al. 2023; Nolan et al. 2020). Inclusion of these biophysical variables in LFMC forecasting may therefore lead to improved forecasts. The core of this new modelling approach is self-supervised learning, e.g. deep neural networks and/or transformers (Requena-Mesa et al. June 2021). This modelling approach poses the impact of climate and weather on the Earth surface as a data-driven, imaged-based, spatio-temporal prediction problem.

A forecasting method proposed by Benson et al. (2024), which utilises this new modelling approach for vegetation productivity, is an ideal candidate approach for forecasting LFMC.

Benson et al.'s model utilises a transformer, artificial intelligence model to leverage the local spatial context and then predict the temporal evolution of small patches of pixels (called 'tokens') using a temporal transformer. Transformer models convert inputs, such as text (e.g. ChatGPT) or images (e.g. ViT), into tokens and use a self-attention mechanism to model how each token relates to all other tokens, enabling the model to efficiently capture both local and global dependencies within the inputs (Dosovitskiy et al. 2021). A temporal transformer tracks these dependencies over time. This approach was enhanced by (Benson et al. 2024) by using a pyramid vision transformer (PVT) which better captures dependencies over multiple spatial scales by dividing the encoding into stages with increasingly larger patches, whereas standard vision transformers have a fixed patch size (Wang et al. 2021). This is important when considering environmental processes like LFMC that are influenced at larger scales by climatic variables and smaller scales by local topography, for example. Here, we explore the suitability of this surface forecasting approach for vegetation processes (Benson et al. 2024) for LFMC forecasting, with some modification including the introduction of a new modelled target variable (i.e. remotely sensed LFMC), and inclusion of biophysical variables.

While Benson et al. (2024) provided a good modelling framework for vegetation forecasting, the importance of individual inputs for the forecast model was not explored. Very few studies using AI models with remote sensing data take an explainable AI approach (Pellicer-Valero et al. 2025), and none to our knowledge for LFMC prediction. With high dimensional models like transformers, simply knowing the trained model weights does not allow assessment of model performance for the right reasons (i.e. what we assume to be important given biophysical understanding of the processes involved, Roscher et al. 2020). Hence the good performance of such a model may be useful but to understand that performance and improve knowledge of the process, i.e. fuel conditions, the application of explainable AI methods must be undertaken. Here we adapt the method of Pellicer-Valero et al. (2025) in applying the Captum Python library to calculate feature attributions with the transformer model via Integrated Gradients (Sundararajan et al. 2017). Feature attribution is a mature branch of explainable AI which aims to explain the positive or negative effect of an input feature on the outcome of the model prediction (Hohl et al. 2024). These approaches overcome the problem of 'black-box' models, a common critique of self-learning approaches (Reichstein et al. 2019), allowing an explanation of the model itself and potential testing of domain specific theory.

In this study we: (i) apply a transformer-based model framework with Sentinel-2 remote sensing, weather and biophysical geospatial data to forecast LFMC, for the first time, across forests of eastern Australia, over a range of lead times (up to 50 days); (ii) test if theory-guided inclusion of biophysical variables and spectral reflectance bands improves model performance; (iii) apply explainable AI methods to understand the influence of model inputs and predictors of LFMC; and (iv) analyse the performance of the LFMC forecasts in tracking known historical drying events. The achievement of these goals in this proof-of-concept modelling study will encourage application of this type of modelling within fire management, including for seasonal fire planning, wildfire preparedness (e.g. timing of prescribed fire), and for responding to wildfires (e.g. resource pre-positioning).

2. Methods

2.1 Study area

The study area encompasses treed areas of the state of New South Wales (NSW), Australia, which spans a wide climatic gradient: temperate to the south, arid to the inland west and subtropical to the coastal north (Figure 1). The largest tracts of forest occur in the coastal lowlands and on the mountain range toward the coastal eastern state edge (maximum elevation ~2000 m.a.s.l.), with widespread patchy woodlands in the arid, flat plains and riverine ecosystems in the centre and west. The area is generally fire prone with frequent low intensity and rarer high-intensity fires occurring during the study period (2015-2025), alongside wet, flooding periods in between (mean rainfall range: <600 mm year^{-1} to >1,500 mm year^{-1}). The predominant forest type is dry sclerophyll forest which comprises eucalypts with shrubby or grassy understories that typically experience fire intervals of between 5-20 years (Murphy et al. 2013; Kenny et al. 2004).

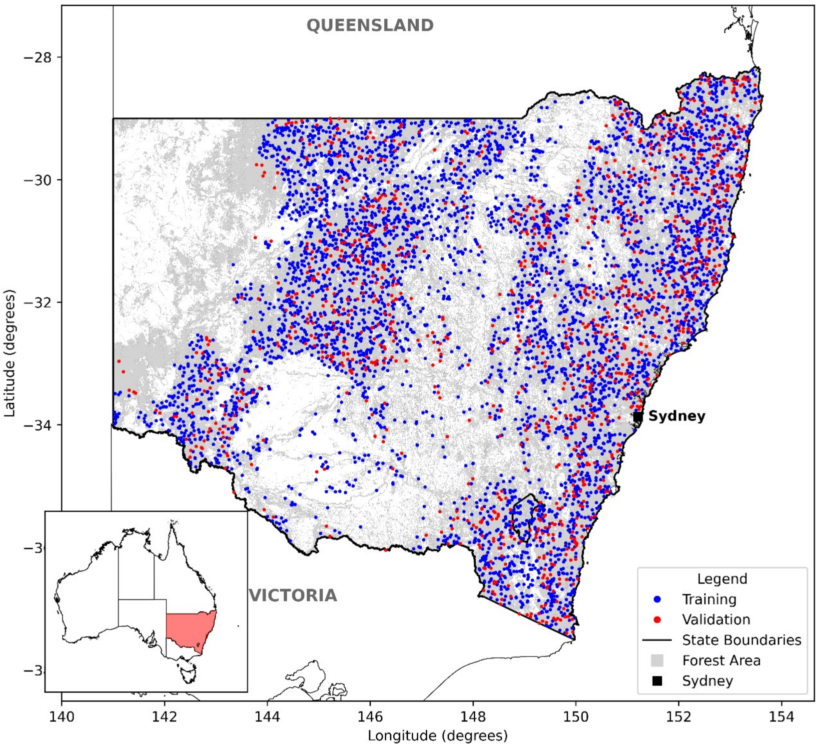

Figure 1. Map of the study area of the state of New South Wales, Australia (inset), with locations of the data minicubes used in LFMC forecast model training (blue) and validation (red). Minicubes were selected to have a minimum of 40% tree-cover pixels (i.e. forest or woodland - grey) over the 2.56 km x 2.56 km area (128 x 128 20 m pixels).

2.2 Minicube dataset in study area

We produced a dataset designed for high resolution vegetation forecasting, for New South Wales (Figure 1). Following Benson et al. (2024) in Europe, the dataset contains not wall-to-wall data but spatio-temporal minicubes of 128 × 128 pixels (2.56 km × 2.56 km) in spatial size by 150 days in daily time steps, including static gridded data on elevation, geomorphology, landcover, vegetation type, and 150 layers of daily meteorology, and 30 layers of 5-daily Sentinel-2 satellite reflectance a (Table 1, see Table S1 for complete sources). The minicube data design ensures a highly diverse training set while keeping the data volume low and hence computational demands manageable. In this study we additionally included variables that are biophysically relevant to spatiotemporal variation in LFMC, namely: additional Sentinel-2 bands, particularly short-wave infrared bands that are sensitive to vegetation water (Yebra et al. 2013); soil moisture which limits plant water uptake (Vinodkumar et al. 2021); vapour pressure deficit which governs plant moisture loss (Griebel et al. 2023); leaf mass per area (LMA) which indicates the dry matter proportion of live fuel (Nolan et al. 2022); vegetation formation which distinguishes among different groupings of species which may have differing water regulation strategies (Jia et al. 2026); and fire history which influences the biomass and physiology of vegetation (McNorton and Di Giuseppe 2024). The minicube variables have two formats: static variables such as elevation or vegetation type, and temporally dynamic variables including Sentinel-2 reflectance and BARRA weather/soil data (BARRA: BOM Atmospheric high-resolution Regional Reanalysis for Australia). Within minicubes, the BARRA data is the only group of variables that exist in the forecast period, prior to prediction of LFMC, and would be actual forecasts in another study whereas here we generate historical predictions, i.e. hind-casting. The meteorology 'forecasts' guide the LFMC predictions in the 50-days forecast period by learning the covariation of LFMC with all predictors in the 100-day training (or context) period. The location of the non-overlapping minicubes was randomly located to capture a wide representation within forests and woodlands, and then additional constraints were applied. Minicubes were selected where 40% or more of the minicube pixels were tree cover, based on an existing product (Fisher et al. 2017), that product being the probability of tree cover based on modelled foliage projective cover classified with supervision from bio-regional thresholds. We also controlled for potential bias created by atmospheric interference, such as cloud, and sampling frequency which depends on the location relative to satellite paths. The cloud mask used was the same deep learning method from the original study (Benson et al. 2024). We randomly selected minicube locations, iteratively allowing the inclusion of minicubes that had fewer observations over time, depending on cloud masking, to prevent the dataset having only locations with frequent good observations (e.g. inland, satellite path overlap). The minicubes were also selected to represent all four calendar seasons. The final dataset included a 3/1 split into training and validation sets, including:

- Training subset: 4,695 minicubes covering 150-day periods in 2015-2023
- Out-of-domain for time validation subset: 1,170 minicubes in separate locations to training in years 2024-2025

For weather and soil data we used the Bureau of Meteorology high-resolution Atmospheric Regional Reanalysis for Australia (BARRA, Su et al. 2025) because of its availability. However, BARRA is not strictly a forecasted weather or environment data stream, rather it is a reanalysis product, making our model a hind-cast. Equivalent true forecasts such as the Australian Community Climate and Earth System Simulator (ACCESS) numerical weather prediction models may suit a potential operationalisation of this method, but its use was beyond the scope of this study due to the cost (Bi et al. 2020). For each BARRA variable we included 3 versions, the mean, minimum and maximum over the 5 days between Sentinel-2 observations, to increase the information available to the self-attention mechanism in the transformer model (Benson et al. 2024).

2.3 Live fuel moisture content prediction

To remotely sense LFMC across the minicubes we used inverse radiative transfer modelling (RTM) based on reflectance data from the Multispectral Instrument onboard the two

Sentinel-2 satellites at 20 m ground resolution (Yebra et al. 2008; Jurdao et al. 2013). The method is described in detail elsewhere (Kotzur et al. 2026). Briefly, an RTM includes forward modelling to simulate the reflectance of leaves and canopies based on biophysical principles and vegetation characteristics, and inverse modelling which uses simulated reflectance to link the characteristics of interest (LFMC in this case) to observed reflectance in the minicubes. From the published forward modelling we filtered the resultant look-up-table (LUT) of simulations, to vegetation type and the leaf area domain of interest and transformed the LUT to match wavelengths of the Sentinel-2 sensor. We inverted the RTM using the spectral angle function and optimised this process based on a validation with field LFMC samples across forests and woodlands of NSW. This resulted in an acceptably accurate model ($R^2 = 0.62$, $p<0.01$, RMSE = 19.92% dry matter content, Kotzur et al. 2026) relative to previous inverse radiative transfer models of the same variable in forests ($R^2 = 0.17$, $p<0.01$, RMSE = 32%, (Yebra et al. 2018). We accepted these error margins and used this LFMC product as the ‘ground truth’ variable in the Contextformer, forecast model of LFMC.

2.4 Contextformer model

The Contextformer model itself is based on Benson et al. (2024) with additional masking and predictor variables. In brief, Contextformer predicts the future vegetation state in terms of NDVI response based on local spatial context patches via a multi-modal transformer. The encoders are a vision transformer for satellite and other static spatial layers, and a multilayer perceptron (MLP) for temporal weather data. This encoding is followed by a temporal transformer processor which fuses the temporal components to the spatial, working on 4 x 4 pixel patches across all timesteps. Lastly a MLP decoder predicts the delta change for a given baseline target value (e.g. last cloud-free value, Kladny et al. 2024). A masked-token-modelling strategy is used to improve generalisation and robustness by switching randomly during training between direct inference (i.e. predicting future timesteps) and random dropout modes (i.e. predicting various context and future timesteps). After the direct inference stage of training the mean absolute error (MAE) was used in the loss functions to penalise the gradients for the next epoch of model training. A maximum of 50 epochs were allowed with the best model chosen based on the root mean squared error (RMSE) between predictions and targets. Whereas Benson et al. (2024) forecasted the whole earth surface within minicubes, in this study we introduced additional masking within the model itself because we were only interested in forecasting LFMC in forests. For each patch, values were only retained if one or more of the 4 pixels was forest, preventing transformer attention or feature learning from non-forest landcovers. The same approach was added to the loss function so that gradients were only calculated from forest pixels, hence non-forest landcovers could not penalise the model for poor prediction in those environments. Another modification from the original model which we found to bias predictions towards zero, was to use non-real mask tokens instead of zero when ingesting the inputs, which were z-score transformed.

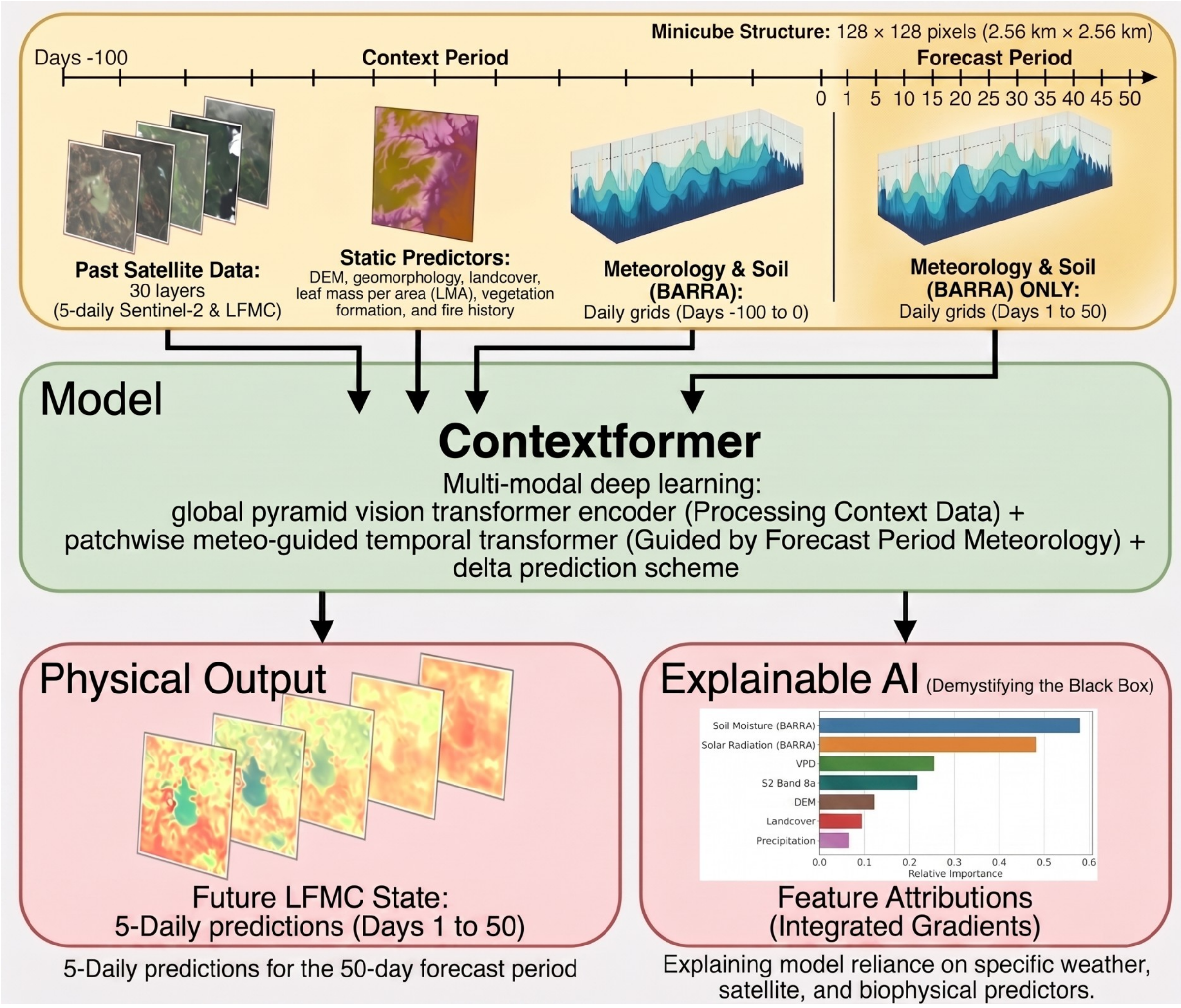

Figure 2. Conceptual model of Contextformer adapted for LFMC from Benson et al. (2024).

2.5 Theory-guided predictor selection

To test if theory-guided predictor selection improves AI model performance we added to the basic weather and reflectance data inputs (Benson et al. 2024), additional reflectance bands, and biophysical LFMC drivers in four different variants (Table 1).

Table 1. Variants of the Contextformer model and the respective inputs and rationales, used in modelling experiment of LFMC forecasting. See Table S1 for complete source information of each predictor in input data.

Model Variant	Input data (all include historical LFMC)	Rationale
0	- 8 BARRA weather variables: mean temp., min. temp., max. temp., precipitation, radiation, air pressure, humidity, wind speed (3 versions of each: 5-day mean, min. and max) - Digital Elevation Model (DEM) - Landcover: Tree cover, Shrubland, Grassland, Cropland, Built-up, Bare/sparse vegetation, Snow and Ice, Permanent water, Herbaceous Wetland, Mangroves, Moss & Lichen - Geomorphons (landforms): flat, summit, ridge, shoulder, spur, slope, hollow, footslope, valley, depression	Simple model focusing on LFMC and dynamic weather/soil moisture BARRA variables, with some static environmental context. We expect this variant of the transformer model Contextformer can forecast LFMC accurately.
1	Variant Model 0 plus: - Sentinel-2 band 2 – blue - Sentinel-2 band 3 – green - Sentinel-2 band 4 – red - Sentinel-2 band 8A – NIR narrow	Inputs from Benson et al. 2025 which describe a general environmental envelope relevant to vegetation processes (e.g. productivity). We expect small improvements in LFMC performance due to additional covariation captured by the Sentinel-2 bands alongside LFMC from the same source.
2	Model 1 plus: - Sentinel-2 band 1 - coastal aerosol - Sentinel-2 band 5 - red edge 1 - Sentinel-2 band 6 - red edge 2 - Sentinel-2 Band 7 - Red Edge 3 - Sentinel-2 band 8 - near infrared (NIR) broad	We expect that the addition of the satellite bands, including 2 shortwave-infrared bands which vary with LFMC, will allow increased information in the fusion of spatial and temporal components within the Contextformer and hence

	- Sentinel-2 band 9 – water vapour - Sentinel-2 band 11 – short-wave infrared (SWIR) 1 - Sentinel-2 band 13 – short-wave infrared (SWIR) 2	improve the weather conditioning of LFMC forecasts.
3	Model 2 plus: - 2 BARRA weather/soil variables: VPD and Soil moisture - Leaf Mass Area (LMA) - Vegetation community - Time since fire - Long term unburnt	We expect that addition of biophysically relevant static inputs will allow the model to better learn the process of LFMC variation and thereby improve the inference of future LFMC.

2.6 Model evaluation

We used common metrics to evaluate the model predictions, both over and throughout the forecast window, such as the Root Mean Squared Error (RMSE), coefficient of determination (R^2) and bias. These metrics were calculated both globally and locally (i.e. all-pixels equally and pixels weighted per minicube). Specifically, global RMSE was weighted by minicube, whereas the global R^2 was evaluated across all valid pixels in all minicubes combined due to the limited number of temporal forecast points within individual forecast windows. Additionally, bias values were reported as absolute metrics to isolate and evaluate systematic over- or under-prediction across the forecast horizon.

We applied explainable AI methods to understand how the model inputs are used in the transformer model. Specifically, we adapt the method of Pellicer-Valero et al. (2025), i.e. the txyXAI Python library, in applying the Captum library for PyTorch to calculate feature attributions of the transformer model via the Integrated Gradients method (Sundararajan et al.

2017, txyXAI v 0.1, Captum v 0.7.0, PyTorch v 2.4.0). Integrated Gradients provides a local explanation for an individual prediction based on input features, which is then summarised for all local attributions across the validation dataset to provide global results. This process is important for LFMC because local drivers will differ between minicube environments across the study area. Integrated Gradients are calculated for an input by shifting from a baseline (e.g. 0) to the actual value and taking the integral of the gradients of the outputs, to answer the question; how much does the deviation of a given feature from historical average change the forecast LFMC compared to the model average prediction of LFMC? Here the choice of baseline is important, so we selected baselines that were consistent with the scaling and physical meaning of each predictor group. We used the implicit baseling in Captum of 0.0 to match the long-term mean of the z-scored predictor groups (i.e. BARRA, static data), while for Sentinel-2, because the reflectance bands were scaled 0-1 we applied an Input Shift which mathematically forces Captum's 0.0 baseline to represent the Sentinel-2 historical mean by shifting the data down by its mean before it enters Captum, and shifting it back up inside the subsequent forward pass of Contextformer. We used the scaled absolute LFMC rather than the delta in the attribution scoring. To enable meaningful comparisons across distinct predictor groups (such as atmospheric weather variables and spectral reflectance bands), we calculated relative attributions by averaging the raw attribution scores for each feature across all validation minicubes and forecast timesteps, and subsequently rescaled these values by multiplying each predictor's attribution by its corresponding input standard deviation to express scores in comparable physical units. In this study, we used this explainable AI approach to understand the model output, not to directly explain the drivers of LFMC. There are likely to be covarying environmental drivers, particularly while using many reflectance bands, hence the predictor attributions were taken as model reliance on certain predictors which may be related to LFMC processes as informed by our ecological understanding of the processes involved (Nolan et al. 2022).

To evaluate the model's capacity to track important fire-risk periods, we performed a targeted trajectory analysis on a subset of minicubes exhibiting large, sustained drying trends within the out-of-domain temporal validation set. For these experiments, minicubes were filtered and randomly selected if they demonstrated a continuous, long-term downward trajectory in target LFMC over the 50-day forecast window. We then plotted the spatial mean and standard deviation of both the target and forecasted LFMC values across each minicube to evaluate temporal alignment. To frame these trajectories within operational fire risk thresholds, performance was benchmarked against a threshold of 60% LFMC. This threshold represents an extreme low moisture level for forests across the New South Wales study region (Nolan et al. 2016). Finally, we assessed the model's predictive asymmetry by comparing its accuracy during these prolonged drying phases against its response to sudden, short-term spikes and drops (i.e. episodic wetting and rapid drying events).

3. Results

3.1 LFMC forecasting model performance

The multi-modal Contextformer model successfully forecasted LFMC across a 50-day window. Predictive performance showed a consistent decline of approximately 30% in accuracy from day 5 to day 50 (Table 2, Figure 3), with the global R^2 dropping from roughly 0.50 to 0.32, while the mean RMSE increased from approximately 14% to nearly 18%. Over all time steps, the global accuracy was promising with R^2 of 0.69, alongside low errors with RMSE of 15.68.

Table 2. Error, accuracy and bias of LFMC forecasts over the 50-day period, from the modelling experiment. Bias is absolute.

Model Variant	Result					
	Global RMSE	Global R^2	Global Bias	RMSE per minicube (median)	R^2 per minicube (median)	Bias per minicube (median)
0: simple model	15.85	**0.69**	9.71	15.09	0.20	0.14
1: vegetation productivity model	15.79	**0.69**	9.72	15.10	0.20	-0.11
2: reflectance-focused model	17.41	0.62	10.73	15.62	0.06	-1.69
3: eco-hydrological model	**15.68**	**0.69**	**9.63**	**14.95**	**0.21**	**0.001**

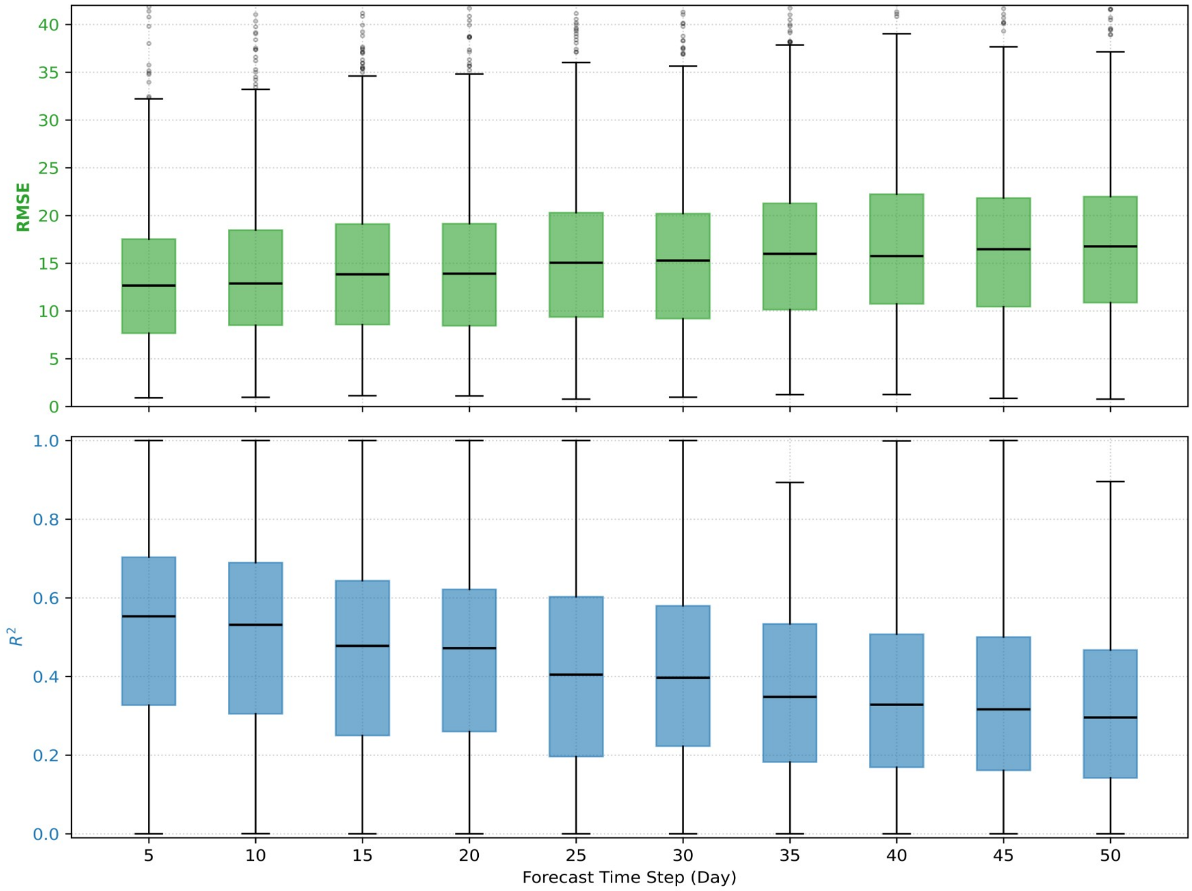

Figure 3. Time series of the distributions of global error (RMSE) and accuracy (R^2) over the LFMC forecast of 50 days (i.e. 10, 5-daily predictions), across the out of domain for time OOD-t validation subset of minicubes.

3.2 Theory-guided predictor selection

Testing different predictor combinations revealed that Model Variant 3 — which had the addition of biophysically targeted inputs like vapour pressure deficit (VPD), soil moisture, and leaf mass per area (LMA) — achieved the lowest overall error (Global RMSE = 15.68%, median RMSE per minicube = 14.95%, Table 2), though the improvement in performance was not large compared to simpler models. Expanding the model only with generic satellite data (Variant 2, adding 8 additional Sentinel-2 bands) did not greatly improve performance, dropping the global R^2 from 0.69 to 0.62 and increasing the median bias from 0.001 to -1.69, highlighting that adding high-dimensional spectral data without explicit biophysical relevance can introduce model noise.

3.3 Explainable AI predictor importance

Global feature attributions calculated via Integrated Gradients demonstrated that the model relies largely on meteorological and soil moisture (BARRA) variables rather than Sentinel-2 reflectance bands to forecast LFMC (Figure 4). Mean and maximum of the average daily temperature emerged as the most important individual drivers determining forecast shifts. Notably, increases in all temperature variables, were strongly attributed to increasing forecasted LFMC, however maximum precipitation also drove positive attributions (increases in LFMC).

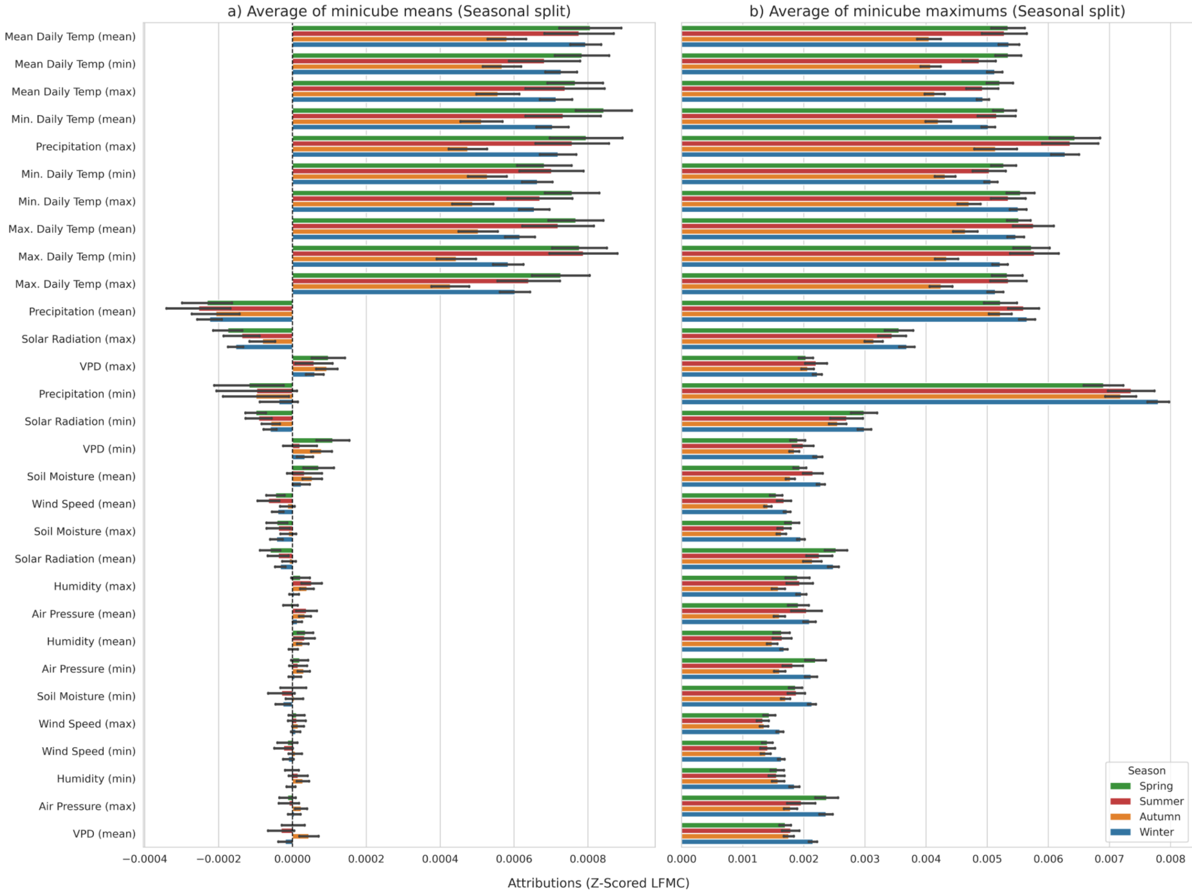

Figure 4. Global mean (a) and local absolute maximum (b) feature attributions by season in the best model of forecasted LFMC (Variant 3) across a random subset of minicubes (n = 390) from the validation subset, across all 50 days of the forecast (i.e. 10, 5-day time steps). Attributions calculated with the Integrated Gradients method in Captum Python library. The local maximum feature attribution is the highest single importance score a feature achieved for any specific localised pixel, time, or prediction (i.e the extreme drivers), whereas the mean regional feature attribution is the average importance of a feature (i.e. the everyday drivers). Positive average importance values indicate an increase in LFMC value, and vice-versa.

3.4 LFMC forecasts for drying minicubes

An analysis of specific out-of-domain minicubes, with the largest observed drying trends over the forecast period, confirmed that the forecasting model effectively tracks sustained, long-term downward trajectories in vegetation moisture (Figure 5). However, the model regularly underpredicts observed short-term temporal fluctuations (as seen in the rapid upward and downward target fluctuations for minicubes 30454 and 30549), signalling a smoother, more conservative trend line in the forecasts. The broad spatial patterns of drying within minicubes were reproduced by the forecasting model (e.g. Figure 5).

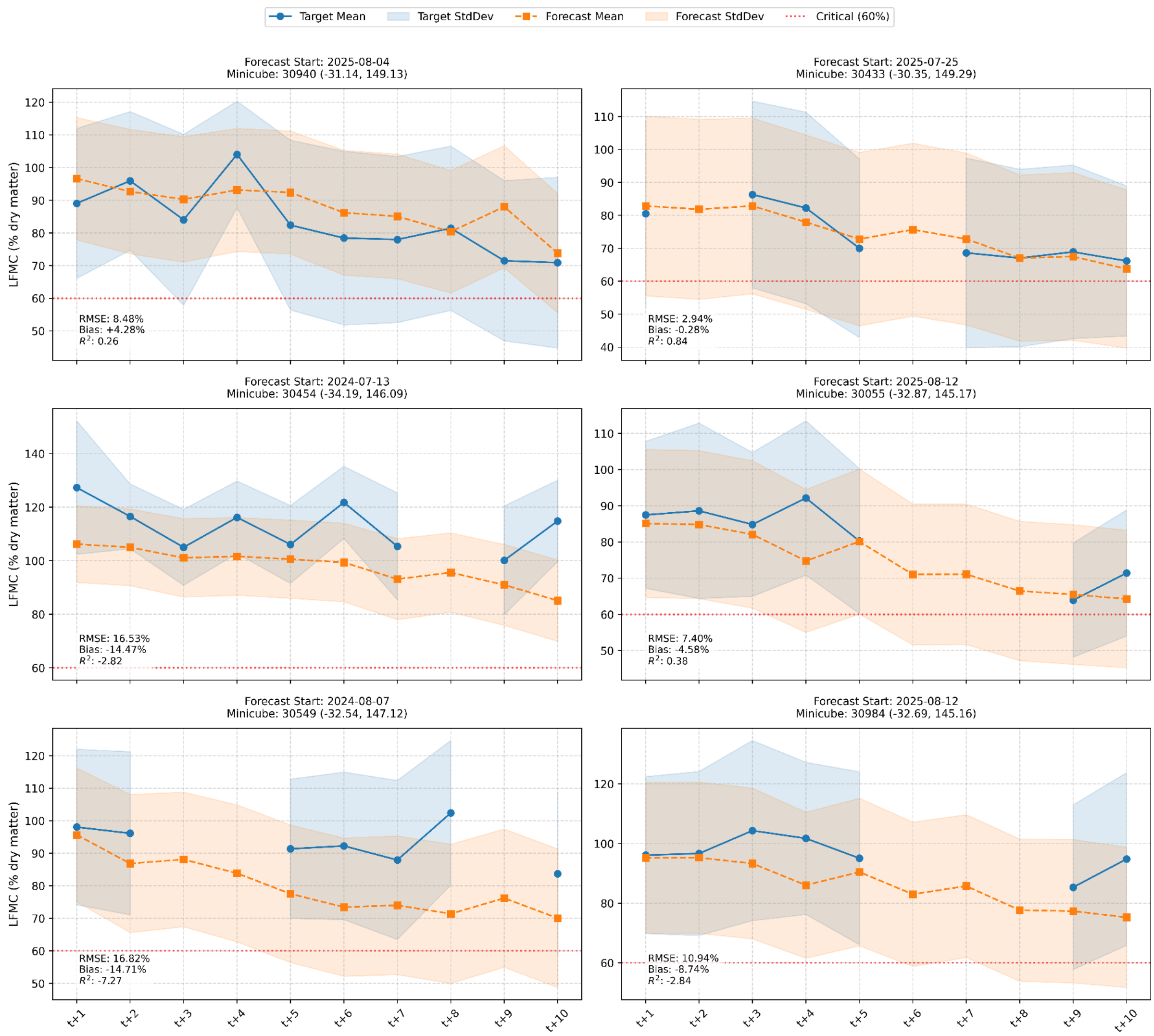

Figure 5: Trajectories of LFMC targets and forecasts of six random minicubes with large drying trends from the OOD-T subset (mean and standard deviation across space of the minicubes). The 60% LFMC marker is a common reference among the plots with different scales, and represents an extreme low LFMC level for forests across the whole dataset and study area.

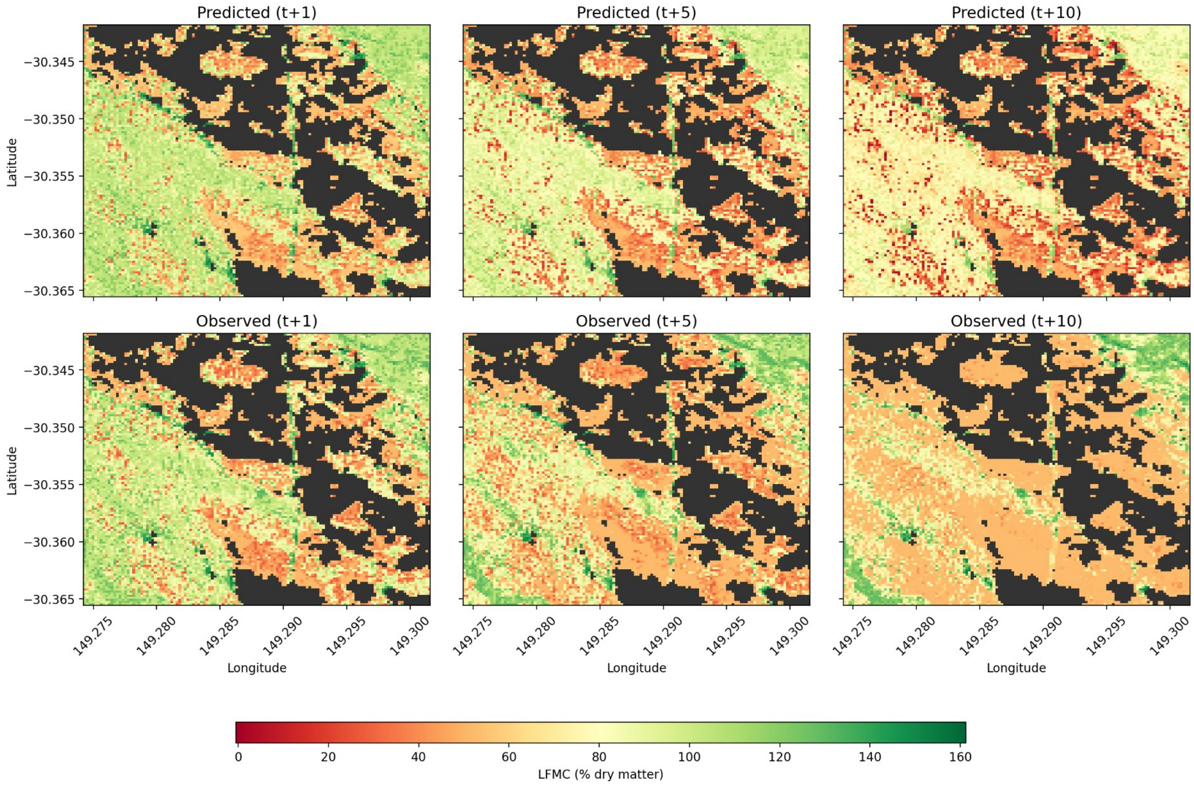

Figure 6. Mapped trajectories of predicted (top) and observed (bottom) LFMC of one minicube with a pronounced drying trend (minicube 30433 from Figure 6), showing 3 of the 10 timesteps from the forecast period (t + 1 & 5 & 10, i.e. forecast days 1 & 25 & 50). The black areas indicate non-forest pixels.

4 Discussion

4.1 LFMC forecasting model performance

As extreme, high-intensity, wildfires become more frequent globally, including in New South Wales (Cunningham et al. 2024), monitoring and forecasting of fine-scale fine fuel conditions becomes important for seasonal planning (Burton et al. 2026). This study successfully meets its primary objective by demonstrating for the first time that transformer-based deep learning architectures can utilise local spatial context to generate forecasts of LFMC across large and diverse forest regions at operationally relevant accuracy, spatial resolution, and lead-times. Given that accuracy degrades linearly over time, land managers and fire authorities could maximise operational utility by running the model continuously on a rolling schedule to focus mostly on the more accurate 5- to 15-day forecast horizons.

An important finding in our evaluation is the divergence between the model's global and local (minicube-level) performance metrics, particularly regarding the coefficient of determination (R^2). While all high-performing model variants achieved a strong global R^2 of approximately 0.69, the median R^2 calculated within individual minicubes dropped significantly to around 0.20–0.21. This disparity is a common statistical artefact of a "restriction of range" when shifting from a regional to a local evaluation scale (Carretta and Ree 2022). Globally, the model evaluates a massive dynamic range of LFMC values across the diverse environments of New South Wales. Because the global metric evaluates all valid pixels in all minicubes combined, it successfully captures this broad, macroscopic spatial variance. Conversely, an individual 2.56 km × 2.56 km minicube usually exhibits relatively homogeneous fuel types and restricted temporal variation over a brief 50-day forecast horizon. Within these localised landscapes, the small total variance compresses the local R^2 score, even though the absolute prediction errors remain low and stable (with median local RMSE values around 14.95% to 15.10%, similar to the global RMSE). This local compression is further compounded by a regression-to-the-mean effect, wherein the transformer model systematically draws its temporal predictions closer to the long-term historical average of the target LFMC variable rather than capturing local, short-term fluctuations in the forecast period. These patterns reveal that while the model is reasonable at capturing absolute localised LFMC levels, its primary statistical strength lies in its capacity to resolve regional-scale macro-climatic gradients across the landscape. This disparity may be due to the coarse spatial resolution of meteorology data not providing enough information at the intra-minicube level, hence limiting the covariation amongst predictors in the context period. Future work should consider different structures or weights amongst the transformer parameters to improve the forecast capability, particularly short-term fluctuations, within minicubes.

4.2 Theory guided predictor selection

While standard black-box AI applications often struggle with generalisation and explainability (Reichstein et al. 2019), this study affirmed that adding additional predictors based on eco-hydrological theory (i.e. Variant 3: VPD, soil moisture, LMA, Vegetation community, Time since fire) provides superior performance over generic inputs. However, the margin of improvement over the simpler model was narrow (Variant 0: basic weather, elevation, land cover and form). This result confirms that while biophysical constraints (like soil moisture and atmospheric VPD) dictate the physiological thresholds of LFMC in forest canopies (Nolan et al. 2020), a temporal transformer can inherently extract the majority of these complex environmental signals directly from macro-meteorology datasets (e.g. BARRA or ACCESS model outputs).

Despite static factors such as LMA, vegetation formation and time-since-fire being included in the best-performing model, as expected (Griebel et al. 2023), these variables are not present in the global feature attributions. This apparent contradiction is a direct consequence of the architecture of the Contextformer model. Because the model uses a delta prediction scheme, the decoder calculates the future state relative to a baseline target value (in this case, the last cloud-free observation, Benson et al. 2024), meaning the initial spatial variation of canopy traits like LMA is already embedded within that starting state. Consequently, the temporal transformer processor prioritises dynamic meteorological or soil drivers (i.e. BARRA data) to compute the directional change across the 50-day window, allowing static biophysical inputs to effectively govern the localised thresholds of the model's environment without showing in the linear pathways measured by feature attribution tools (Pellicer-Valero et al. 2025).

4.3 Explainable AI predictor importance

By integrating feature attribution tools, this research addresses a major critique of deep-learning architectures in ecological modelling (Reichstein et al. 2019). The global attribution results prove that the future LFMC model is consistent with basic plant eco-physiological knowledge (Qi et al. 2012): it actively relies on air temperature and precipitation to establish future LFMC states, with the best model, Variant 3, being slightly superior because its inputs included soil moisture, which had small feature importances, and other static biophysically relevant predictors. The latter may constrain the baseline starting state more accurately, but the importances were unable to be quantified due to the model structure (see Methods). However, the negligible attribution score of Sentinel-2 spectral bands suggests that while remote sensing is vital for predicting the initial "ground truth" LFMC, weather variations completely dominate the LFMC trend over multi-week forecast windows. That is, the covariation between reflectance bands, LFMC and biophysical predictors is negligible compared to variation between LFMC and the biophysical predictors. However, it must be noted that the Sentinel-2 data only exists in the context period of the mini-cube (the first 100 of 150 days), while BARRA weather data extends into the 'future' (final 50 days), hence the BARRA weathers are more likely to influence forecasted LFMC in the same 'future' period. Without forecasted reflectance data there is likely to be a structural bias against the importance of reflectance bands on the forecast LFMC.

A notable finding within the feature attributions is the positive role of air temperature. It drives a strong effect on the forecast in the global signed attributions (Figure 4) and placed high in the maximum absolute attribution plot (Figure 5), showing that it is the most powerful overall predictor the model relies upon to determine future LFMC, followed by rainfall. While a positive global relationship between air temperature and fuel dryness may seem counterintuitive from a steady-state plant biophysics perspective, this behaviour reflects how Contextformer can explicate indirect relationships, particularly the seasonal increase in air temperature resulting in vegetation growth pulses hence increases in the fraction of juvenile leaves in tree canopies resulting in increases in landscape LFMC. The attribution scores are largest in spring for the majority of temperature variables, with a few being largest in summer. Furthermore, other important predictors had the direction and size of attribution on forecasted LFMC expected by eco-hydrological theory (Nolan et al. 2020), for example large positive average influence of maximum rainfall, moderate negative average influence of solar radiation, and the very large absolute influence of minimum rainfall (i.e. the deep rehydration of soils hence vegetation following prolonged wet spells, Figure 4). These results suggest that the transformer model has made predictions using overarching drivers and relied less on the more direct LFMC drivers like VPD and soil moisture had lesser influence than is expected. This suppression of derived indices is likely exacerbated by the mathematical mechanics of the attribution method, where collinearity causes primary meteorological drivers to absorb the attribution scores of highly correlated secondary variables like VPD and soil moisture. Previous continental-scale analyses across Australia have established that soil moisture serves as a strong indicator for LFMC over lagged intervals of days to months (Vinodkumar et al. 2021), however we did not find that, here, because of the capacity of the transformer and the co-linearity of soil moisture with other more influential predictors such as rainfall.

This study has successfully demonstrated that LFMC can be reliably forecasted using temporal transformer models and targeted biophysical predictors. Naturally, to operationalise this framework, several practical caveats must be addressed. First, the model would require predictor data available up to the present with minimal latency, replacing the BARRA reanalysis data with genuine weather forecasts (such as the ACCESS numerical weather prediction models). Consequently, the model would need to include the inherent uncertainty of unadjusted weather forecasts, which could propagate errors and influence the predictive performance observed in this historical study. Furthermore, operationalising the model over continuous, large-scale areas would necessitate the generation of significantly more minicubes, resulting in massive data volumes due to the numerous high-resolution predictors required for each 50-day forecast horizon. However, these challenges are entirely manageable using modern high-performance cloud computing infrastructure, automated Earth observation data pipelines, and optimised data management workflows to handle real-time ingestion.

4.4 LFMC forecasts for drying minicubes

The model's tendency to confidently predict LFMC drying trajectories while somewhat underestimating sudden wetting events can be explained partly by data imbalances; natural forest ecosystems spend prolonged periods steadily drying out, punctuated by rapid, episodic rain events. While this asymmetry means short-term recoveries might be missed, the model remains effective at capturing prolonged drying or "dieback" phases where fuel hazards peak. Additionally, the short-term positive increases in the remotely sensed LFMC ground truth (Figure 5), may sometimes be caused by clouds undetected in the masking process rather than by actual 10- to 15-day wetting periods. If operationalising this model, these artefacts should be accounted for by quality control and possibly further cloud masking. Researchers should also note, that these forecasts remain inherently capped by the baseline LFMC accuracy (R^2=0.62) of the underlying radiative transfer models used to train it (Kotzur et al. 2026), meaning future improvements to satellite-derived LFMC mapping will inherently yield better forecasting systems.

Conflicts of interest

The authors declare that they have no conflicts of interest.

Declaration of funding

This research was supported by funding from the New South Wales government via the NSW Bushfire and Natural Hazards Research Centre, and an Australian Research Council Linkage Grant (LP190100436).

Data availability

The dataset of spatiotemporal minicubes and code for the adapted Contextformer model are available on request. BARRA reanalysis data were sourced from the Bureau of Meteorology via the Data Catalogue of the National Computational Infrastructure (NCI).

Author contributions

IK: Conceptualization, Methodology, Software, Data Curation, Formal Analysis, Writing – Original Draft. MB: Conceptualization, Supervision, Writing – Review & Editing. RN: Conceptualization, Supervision, Funding Acquisition, Writing – Review & Editing. VB: Analysis, Writing – Review & Editing.

Declaration of use of AI

Artificial intelligence models (transformers) were used as the core predictive modelling framework in this research. Large language models were used for editing assistance during manuscript preparation.

References

Abatzoglou JT and Williams AP (2016) 'Impact of anthropogenic climate change on wildfire across western US forests', *Proceedings of the National Academy of Sciences*, 113(42):11770–11775, doi:10.1073/pnas.1607171113.

Abram NJ, Henley BJ, Sen Gupta A, Lippmann TJR, Clarke H, Dowdy AJ, Sharples JJ, Nolan RH, Zhang T, Wooster MJ, Wurtzel JB, Meissner KJ, Pitman AJ, Ukkola AM, Murphy BP, Tapper NJ and Boer MM (2021) 'Connections of climate change and variability to large and extreme forest fires in southeast Australia', *Communications Earth & Environment*, 2(1):8, doi:10.1038/s43247-020-00065-8.

Alexander ME and Cruz MG (2012) 'Assessing the effect of foliar moisture on the spread rate of crown fires', *International Journal of Wildland Fire*, 22(4):415–427, doi:10.1071/WF12008.

Argañaraz JP, Landi MA, Scavuzzo CM and Bellis LM (2018) ‘Determining fuel moisture thresholds to assess wildfire hazard: A contribution to an operational early warning system’, *PLOS ONE*, 13(10):e0204889, doi:10.1371/journal.pone.0204889.

Banerjee T (2026) ‘The Role of Canopy Turbulence in Wildland Fire Behavior’, *Annual Review of Fluid Mechanics*, 58(Volume 58, 2026):473–502, doi:10.1146/annurev-fluid-112723-062216.

Benson V, Robin C, Requena-Mesa C, Alonso L, Carvalhais N, Cortés J, Gao Z, Linscheid N, Weynants M and Reichstein M (2024) ‘Multi-Modal Learning for Geospatial Vegetation Forecasting’, in *2024 IEEE/CVF Conference on Computer Vision and Pattern Recognition (CVPR)*, *2024 IEEE/CVF Conference on Computer Vision and Pattern Recognition (CVPR)*, IEEE, Seattle, WA, USA, doi:10.1109/CVPR52733.2024.02625.

Bi D, Dix M, Marsland S, O’Farrell S, Sullivan A, Bodman R, Law R, Harman I, Srbinovsky J, Rashid HA, Dobrohotoff P, Mackallah C, Yan H, Hirst A, Savita A, Dias FB, Woodhouse M, Fiedler R and Heerdegen A (2020) ‘Configuration and spin-up of ACCESS-CM2, the new generation Australian Community Climate and Earth System Simulator Coupled Model’, *Journal of Southern Hemisphere Earth Systems Science*, 70(1):225–251, doi:10.1071/ES19040.

Burton JE, Collins L, Nolan RH, Clarke H, Penman TD, Cirulis BA and Cawson JG (2026) ‘Metrics into management: which measures of landscape moisture best inform wildfire planning and response?’, *International Journal of Wildland Fire*, 35(8):WF25233, doi:10.1071/WF25233.

Carretta TR and Ree MJ (2022) ‘Correction for range restriction: Lessons from 20 research scenarios’, *Military Psychology*, 34(5):551–569, doi:10.1080/08995605.2021.2022067.

Chuvieco E, Cocero D, Riaño D, Martin P, Martínez-Vega J, de la Riva J and Pérez F (2004) ‘Combining NDVI and surface temperature for the estimation of live fuel moisture content in forest fire danger rating’, *Remote Sensing of Environment*, 92(3):322–331, doi:10.1016/j.rse.2004.01.019.

Costa-Saura JM, Balaguer-Beser Á, Ruiz LA, Pardo-Pascual JE and Soriano-Sancho JL (2021) ‘Empirical models for spatio-temporal live fuel moisture content estimation in mixed mediterranean vegetation areas using sentinel-2 indices and meteorological data’, *Remote Sensing*, 13(18), doi:10.3390/rs13183726.

Cunningham CX, Williamson GJ and Bowman DMJS (2024) ‘Increasing frequency and intensity of the most extreme wildfires on Earth’, *Nature Ecology & Evolution*, 8(8):1420–1425, doi:10.1038/s41559-024-02452-2.

Dennison PE and Moritz MA (2009) ‘Critical live fuel moisture in chaparral ecosystems: a threshold for fire activity and its relationship to antecedent precipitation’, *International Journal of Wildland Fire*, 18(8):1021–1027, doi:10.1071/WF08055.

Dimitrakopoulos AP and Bemmerzouk AM (2003) ‘Predicting live herbaceous moisturecontent from a seasonal drought index’, *International Journal of Biometeorology*, 47(2):73–79, doi:10.1007/s00484-002-0151-1.

Dosovitskiy A, Beyer L, Kolesnikov A, Weissenborn D, Zhai X, Unterthiner T, Dehghani M, Minderer M, Heigold G, Gelly S, Uszkoreit J and Houlsby N (2021) ‘An Image is Worth 16x16 Words: Transformers for Image Recognition at Scale’, doi:10.48550/arXiv.2010.11929.

Ellis W, Melzer A, Green B, Newgrain K, Hindell M and Carrick F (1995) ‘Seasonal-Variation in Water Flux, Field Metabolic-Rate and Food-Consumption of Free-Ranging Koalas (Phascolarctos-Cinereus)’, *Australian Journal of Zoology*, 43(1):59, doi:10.1071/ZO9950059.

Fisher A, Danaher T and Gill T (2017) ‘Mapping trees in high resolution imagery across large areas using locally variable thresholds guided by medium resolution tree maps’, *International Journal of Applied Earth Observation and Geoinformation*, 58:86–96, doi:10.1016/j.jag.2017.02.004.

García M, Chuvieco E, Nieto H and Aguado I (2008) ‘Combining AVHRR and meteorological data for estimating live fuel moisture content’, *Remote Sensing of Environment*, 112(9):3618–3627, doi:10.1016/j.rse.2008.05.002.

Griebel A, Boer MM, Blackman C, Choat B, Ellsworth DS, Madden P, Medlyn B, Resco de Dios V, Wujeska-Klause A, Yebra M, Younes Cardenas N and Nolan RH (2023) ‘Specific leaf area and vapour pressure deficit control live fuel moisture content’, *Functional Ecology*, 37(3):719–731, doi:10.1111/1365-2435.14271.

Hohl A, Obadic I, Fernández-Torres M-Á, Najjar H, Oliveira DAB, Akata Z, Dengel A and Zhu XX (2024) ‘Opening the Black Box: A systematic review on explainable artificial intelligence in remote sensing’, *IEEE Geoscience and Remote Sensing Magazine*, 12(4):261–304, doi:10.1109/MGRS.2024.3467001.

Jain P, Barber QE, Taylor SW, Whitman E, Castellanos Acuna D, Boulanger Y, Chavardès RD, Chen J, Englefield P, Flannigan M, Girardin MP, Hanes CC, Little J, Morrison K, Skakun RS, Thompson DK, Wang X and Parisien M-A (2024) ‘Drivers and Impacts of the Record-Breaking 2023 Wildfire Season in Canada’, *Nature Communications*, 15(1):6764, doi:10.1038/s41467-024-51154-7.

Jia Q, Quan X, Resco De Dios V, Yebra M, He B, Li X, Liao Z, Balaguer-Romano R and De Cáceres M (2026) ‘Enhancing two-week live fuel moisture content forecasts through biophysical modelling and remote sensing data assimilation’, *Remote Sensing of Environment*, 335:115267, doi:10.1016/j.rse.2026.115267.

Jurdao S, Yebra M, Guerschman JP and Chuvieco E (2013) ‘Regional estimation of woodland moisture content by inverting Radiative Transfer Models’, *Remote Sensing of Environment*, 132:59–70, doi:10.1016/j.rse.2013.01.004.

Kenny B, Sutherland E, Tasker E and Bradstock R (2004) 'Guidelines for ecologically sustainable fire management', *NSW National Parks and Wildlife Service, Hurstville*.

Kladny K-R, Milanta M, Mraz O, Hufkens K and Stocker BD (2024) 'Enhanced prediction of vegetation responses to extreme drought using deep learning and Earth observation data', *Ecological Informatics*, 80:102474, doi:10.1016/j.ecoinf.2024.102474.

Kotzur I (2024) *On the environmental dynamics of forests, koala habitat and climate refugia in eastern Australia: a remote sensing approach* [Ph.D. Thesis], Western Sydney University.

Kotzur I, Boer M, Yebra M and Moore BD (2026) 'Monitoring Forest Foliar Moisture Using Sentinel-2 Reflectance and Radiative Transfer Model Inversion in Australia', *IEEE Journal of Selected Topics in Applied Earth Observations and Remote Sensing*1–18, doi:10.1109/JSTARS.2026.3704632.

Matthews S (2013) 'Dead fuel moisture research: 1991–2012', *International Journal of Wildland Fire*, 23(1):78–92, doi:10.1071/WF13005.

McNorton JR and Di Giuseppe F (2024) 'A global fuel characteristic model and dataset for wildfire prediction', *Biogeosciences*, 21(1):279–300, doi:10.5194/bg-21-279-2024.

Mella VSA, McArthur C, Krockenberger MB, Frend R and Crowther MS (2019) 'Needing a drink: Rainfall and temperature drive the use of free water by a threatened arboreal folivore', *PLoS ONE*, 14(5):1–16, doi:10.1371/journal.pone.0216964.

Murphy BP, Bradstock RA, Boer MM, Carter J, Cary GJ, Cochrane MA, Fensham RJ, Russell-Smith J, Williamson GJ and Bowman DMJS (2013) 'Fire regimes of Australia: A pyrogeographic model system', *Journal of Biogeography*, 40(6):1048–1058, doi:10.1111/jbi.12065.

Nolan RH, Blackman CJ, de Dios VR, Choat B, Medlyn BE, Li X, Bradstock RA and Boer MM (2020) 'Linking Forest Flammability and Plant Vulnerability to Drought', *Forests*, 11(7):779, doi:10.3390/f11070779.

Nolan RH, Boer MM, Resco de Dios V, Caccamo G and Bradstock RA (2016) 'Large-scale, dynamic transformations in fuel moisture drive wildfire activity across southeastern Australia', *Geophysical Research Letters*, 43(9):4229–4238, doi:10.1002/2016GL068614.

Nolan RH, Foster B, Griebel A, Choat B, Medlyn BE, Yebra M, Younes N and Boer MM (2022) 'Drought-related leaf functional traits control spatial and temporal dynamics of live fuel moisture content', *Agricultural and Forest Meteorology*, 319(December 2021):108941, doi:10.1016/j.agrformet.2022.108941.

Pellicer-Valero OJ, Fernández-Torres M-Á, Chaonan Ji, Mahecha MD and Camps-Valls G (2025) 'Explainable Earth Surface Forecasting Under Extreme Events', *Earth's Future*, 13(9):e2024EF005446, doi:10.1029/2024EF005446.

Qi Y, Dennison PE, Spencer J and Riaño D (2012) ‘Monitoring Live Fuel Moisture Using Soil Moisture and Remote Sensing Proxies’, *Fire Ecology*, 8(3):71–87, doi:10.4996/fireecology.0803071.

Quan X, Boer MM, Nolan RH, He B, Bendall E, Gibson R, Carnegie AJ and Choat B (2026) ‘Quantifying the 2023 sudden forest canopy dieback event in southeastern Australia using ground-based surveys and Sentinel-2-derived live fuel moisture content’, *Agricultural and Forest Meteorology*, 387:111290, doi:10.1016/j.agrformet.2026.111290.

Quan X, Chen R, Yebra M, Riaño D, Resco de Dios V, Li X, He B, Nolan RH, Griebel A, Boer MM and Sun Y (2024) ‘Sub-daily live fuel moisture content estimation from Himawari-8 data’, *Remote Sensing of Environment*, 308, doi:10.1016/j.rse.2024.114170.

Quan X, Yebra M, Riaño D, He B, Lai G and Liu X (2021) ‘Global fuel moisture content mapping from MODIS’, *International Journal of Applied Earth Observation and Geoinformation*, 101:102354, doi:10.1016/j.jag.2021.102354.

Reichstein M, Camps-Valls G, Stevens B, Jung M, Denzler J, Carvalhais N and Prabhat (2019) ‘Deep learning and process understanding for data-driven Earth system science’, *Nature*, 566(7743):195–204, doi:10.1038/s41586-019-0912-1.

Requena-Mesa C, Benson V, Reichstein M, Runge J and Denzler J (June 2021) ‘EarthNet2021: A large-scale dataset and challenge for Earth surface forecasting as a guided video prediction task’, in *2021 IEEE/CVF Conference on Computer Vision and Pattern Recognition Workshops (CVPRW)*, *2021 IEEE/CVF Conference on Computer Vision and Pattern Recognition Workshops (CVPRW)*, IEEE, Nashville, TN, USA, doi:10.1109/CVPRW53098.2021.00124.

Roscher R, Bohn B, Duarte MF and Garcke J (2020) ‘Explainable Machine Learning for Scientific Insights and Discoveries’, *IEEE Access*, 8:42200–42216, doi:10.1109/ACCESS.2020.2976199.

Rossa CG and Fernandes PM (2018) ‘Live fuel moisture content: The “pea under the mattress” of fire spread rate modeling?’, *Fire*, 1(3):1–5, doi:10.3390/fire1030043.

Ruthrof KX, Fontaine JB, Matusick G, Breshears DD, Law DJ, Powell S and Hardy G (2016) ‘How drought-induced forest die-off alters microclimate and increases fuel loadings and fire potentials’, *International Journal of Wildland Fire*, 25(8):819–830, doi:10.1071/WF15028.

Santos FLM, Couto FT, Monteiro MJ, Ribeiro NA, Le Moigne P and Salgado R (2026) ‘Seasonal prediction of live fuel moisture content’, *Journal of Pyrogeography*, 2(1):100010, doi:10.1016/j.pyro.2026.100010.

Su C-H, Torrance J, Rennie S, Howard E, Stassen C, Warren R, Smith A, Dharssi I, Pepler A, Tian S, Lipson M, Steinle P, Franklin C, Le T, Wang C, Masoumi S and Le Marshall J (2025) ‘The Australian regional atmospheric reanalysis system, version 2 – BARRA2’, *Journal of Southern Hemisphere Earth Systems Science*, 75(3):ES25032, doi:10.1071/ES25032.

Sundararajan M, Taly A and Yan Q (2017) 'Axiomatic Attribution for Deep Networks', doi:10.48550/arXiv.1703.01365.

Viegas DX, Piñol J, Viegas MT and Ogaya R (2001) 'Estimating live fine fuels moisture content using meteorologically-based indices', *International Journal of Wildland Fire*, 10(2):223–240, doi:10.1071/WF01022.

Vinodkumar V, Dharssi I, Yebra M and Fox-Hughes P (2021) 'Continental-scale prediction of live fuel moisture content using soil moisture information', *Agricultural and Forest Meteorology*, 307(January):108503, doi:10.1016/j.agrformet.2021.108503.

Wang W and Quan X (2023) 'Estimation of Live Fuel Moisture Content From Multiple Sources of Remotely Sensed Data', *IEEE Geoscience and Remote Sensing Letters*, 20:1–5, doi:10.1109/LGRS.2023.3291718.

Wang W, Xie E, Li X, Fan D-P, Song K, Liang D, Lu T, Luo P and Shao L (2021) 'Pyramid Vision Transformer: A Versatile Backbone for Dense Prediction without Convolutions', in *2021 IEEE/CVF International Conference on Computer Vision (ICCV)*, *2021 IEEE/CVF International Conference on Computer Vision (ICCV)*, IEEE, Montreal, QC, Canada, doi:10.1109/ICCV48922.2021.00061.

Watt MS, Gross S, Difuntorum JK, McCarty JL, Pearce HG, Shuman JK and Yebra M (2025) 'Monitoring Wildfire Risk with a Near-Real-Time Live Fuel Moisture Content System: A Review and Roadmap for Operational Application in New Zealand', *Remote Sensing*, 17(21), doi:10.3390/rs17213580.

Yebra M, Chuvieco E and Riaño D (2008) 'Estimation of live fuel moisture content from MODIS images for fire risk assessment', *Agricultural and Forest Meteorology*, 148(4):523–536, doi:10.1016/j.agrformet.2007.12.005.

Yebra M, Dennison PE, Chuvieco E, Riaño D, Zylstra P, Hunt ER, Danson FM, Qi Y and Jurdao S (2013) 'A global review of remote sensing of live fuel moisture content for fire danger assessment: Moving towards operational products', *Remote Sensing of Environment*, doi:10.1016/j.rse.2013.05.029.

Yebra M, Quan X, Riaño D, Rozas Larraondo P, van Dijk AIJM and Cary GJ (2018) 'A fuel moisture content and flammability monitoring methodology for continental Australia based on optical remote sensing', *Remote Sensing of Environment*, 212(November 2017):260–272, doi:10.1016/j.rse.2018.04.053.

Yebra M, Scortechini G, Younes N and Dijk AIJM van (2026) 'High-Resolution Monitoring of Live Fuel Moisture Content Across Australia', *Remote Sensing*, 18(7), doi:10.3390/rs18071049.

Table S1. Variables used in Contextformer Vision Transformer model to forecast Live Fuel Moisture Content in forests of NSW.

Variable	Units	Native Resolution	Source	Use
Live fuel moisture content (LFMC) modelled from Sentinel-2	% dry matter	20 m	Kotzur et al. (2026)	Target variable
Sentinel-2 scene classification	Nominal	20 m	European Space Agency (Drusch et al. 2012) via Planetary Computer	Quality control
Sentinel-2 band 1 - coastal aerosol	%	60 m		Predictor variable
Sentinel-2 band 2 – blue	%	10 m		Predictor variable
Sentinel-2 band 3 – green	%	10 m		Predictor variable
Sentinel-2 band 4 – red	%	10 m		Predictor variable
Sentinel-2 band 5 - red edge 1	%	20 m		Predictor variable
Sentinel-2 band 6 - red edge 2	%	20 m		Predictor variable
Sentinel-2 Band 7 - Red Edge 3	%	20 m		Predictor variable
Sentinel-2 band 8 - near infrared (NIR) broad	%	10 m		Predictor variable
Sentinel-2 band 8A - near infrared (NIR) narrow	%	20 m		Predictor variable
Sentinel-2 band 9 – water vapour	%	60 m		Predictor variable
Sentinel-2 band 11 – short-wave infrared (SWIR) 1	%	20 m		Predictor variable
Sentinel-2 band 13 – short-wave infrared (SWIR) 2	%	20 m		Predictor variable
Cloud deep learning mask (Sentinel-2)	Nominal	20 m	(Benson et al. 2024)	Quality control and masked-token-modelling
Mean daily temperature	ºC	~4.4 km	BARRA (Su et al. 2025)	Predictor variable
Minimum daily temperature	ºC			Predictor variable

Maximum daily	ºC			Predictor variable
Mean daily near-surface wind speed	m s^{-1}			Predictor variable
Precipitation	mm d^{-1}			Predictor variable
Mean daily air pressure at sea level	hPa			Predictor variable
Mean daily near-surface relative humidity	%			Predictor variable
Mean daily surface downwelling shortwave radiation	W m^{-2}			Predictor variable
Mean daily total soil moisture content (0-3 m)	kg m^{-2}			Predictor variable
Mean daily vapour pressure deficit	kPa		Derived (from BARRA): *es = 0.6108 * np.exp(17.27 * Max.Temp / (Max.Temp + 237.3))* *ea = (Rel.Hum / 100) * es* *VPD = es - ea*	Predictor variable
ALOS World Digital Elevation Model (DEM)	M	30 m	Japan Aerospace Exploration Agency (Takaku et al. 2021) via Planetary Computer	Predictor variable
ESA World Cover Landcover	Nominal	10 m	European Space Agency (Zanaga et al. 2022) via Planetary Computer	Forest mask and Quality Control
Geomorphons (topographic	Nominal	90 m	(Amatulli et al. 2020) via	Predictor variable

classes)			Planetary Computer	
Leaf mass per area (LMA)	kg m^{-2}	10 km	(Andrew et al. 2025; Falster et al. 2021)	Predictor variable
Vegetation community type	Nominal	5 m	NSW State Government (Roff et al. 2022)	Predictor variable (NSW Vegetation Formation)
Time since fire	D	Vector	NSW and NPWS Fire Histories (DPIE 2026; National Bushfire Intelligence Capability 2026) via SEED	Predictor variable
Long term unburnt or unknown fire history	Boolean	Vector		Predictor variable

References

Amatulli G, McInerney D, Sethi T, Strobl P and Domisch S (2020) ‘Geomorpho90m, empirical evaluation and accuracy assessment of global high-resolution geomorphometric layers’, *Scientific Data*, 7(1):162, doi:10.1038/s41597-020-0479-6.

Andrew SC, Martín-Forés I, Guerin GR, Coleman D, Falster DS, Wenk E, Wright IJ and Gallagher RV (2025) ‘Mapping Plant Functional Traits Using Gap-Filled Datasets to Inform Management and Modelling’, *Global Ecology and Biogeography*, 34(10):e70136, doi:10.1111/geb.70136.

Benson V, Robin C, Requena-Mesa C, Alonso L, Carvalhais N, Cortés J, Gao Z, Linscheid N, Weynants M and Reichstein M (2024) ‘Multi-Modal Learning for Geospatial Vegetation Forecasting’, in *2024 IEEE/CVF Conference on Computer Vision and Pattern Recognition (CVPR)*, *2024 IEEE/CVF Conference on Computer Vision and Pattern Recognition (CVPR)*, IEEE, Seattle, WA, USA, doi:10.1109/CVPR52733.2024.02625.

DPIE (2026) ‘NPWS Fire History - Wildfires and Prescribed Burns’, https://datasets.seed.nsw.gov.au/dataset/fire-history-wildfires-and-prescribed-burns-1e8b6.

Drusch M, Del Bello U, Carlier S, Colin O, Fernandez V, Gascon F, Hoersch B, Isola C, Laberinti P, Martimort P, Meygret A, Spoto F, Sy O, Marchese F and Bargellini P (2012) ‘Sentinel-2: ESA’s Optical High-Resolution Mission for GMES Operational Services’, *Remote Sensing of Environment*, 120:25–36, doi:10.1016/j.rse.2011.11.026.

Falster D, Gallagher R, Wenk EH, Wright IJ, Indiarto D, Andrew SC, Baxter C, Lawson J, Allen S, Fuchs A, Monro A, Kar F, Adams MA, Ahrens CW, Alfonzetti M, Angevin T, Apgaua DMG, Arndt S, Atkin OK, Atkinson J, Auld T, Baker A, von Balthazar M, Bean A, Blackman CJ, Bloomfield K, Bowman DMJS, Bragg J, Brodribb TJ, Buckton G, Burrows G, Caldwell E, Camac J, Carpenter R, Catford JA, Cawthray GR, Cernusak LA, Chandler G, Chapman AR, Cheal D, Cheesman AW, Chen S-C, Choat B, Clinton B, Clode PL, Coleman H, Cornwell WK, Cosgrove M, Crisp M, Cross E, Crous KY, Cunningham S, Curran T, Curtis E, Daws MI, DeGabriel JL, Denton MD, Dong N, Du P, Duan H, Duncan DH, Duncan RP, Duretto M, Dwyer JM, Edwards C, Esperon-Rodriguez M, Evans JR, Everingham SE, Farrell C, Firn J, Fonseca CR, French BJ, Frood D, Funk JL, Geange SR, Ghannoum O, Gleason SM, Gosper CR, Gray E, Groom PK, Grootemaat S, Gross C, Guerin G, Guja L, Hahs AK, Harrison MT, Hayes PE, Henery M, Hochuli D, Howell J, Huang G, Hughes L, Huisman J, Ilic J, Jagdish A, Jin D, Jordan G, Jurado E, Kanowski J, Kasel S, Kellermann J, Kenny B, Kohout M, Kooyman RM, Kotowska MM, Lai HR, Laliberté E, Lambers H, Lamont BB, Lanfear R, van Langevelde F, Laughlin DC, Laugier-Kitchener B-A, Laurance S, Lehmann CER, Leigh A, Leishman MR, Lenz T, Lepschi B, Lewis JD, Lim F, Liu U, Lord J, Lusk CH, Macinnis-Ng C, McPherson H, Magallón S, Manea A, López-Martinez A, Mayfield M, McCarthy JK, Meers T, van der Merwe M, Metcalfe DJ, Milberg P, Mokany K, Moles AT, Moore BD, Moore N, Morgan JW, Morris W, Muir A, Munroe S, Nicholson Á, Nicolle D, Nicotra AB, Niinemets Ü, North T, O'Reilly-Nugent A, O'Sullivan OS, Oberle B, Onoda Y, Ooi MKJ, Osborne CP, Paczkowska G, Pekin B, Guilherme Pereira C, Pickering C, Pickup M, Pollock LJ, Poot P, Powell JR, Power SA, Prentice IC, Prior L, Prober SM, Read J, Reynolds V, Richards AE, Richardson B, Roderick ML, Rosell JA, Rossetto M, Rye B, Rymer PD, Sams MA, Sanson G, Sauquet H, Schmidt S, Schönenberger J, Schulze E-D, Sendall K, Sinclair S, Smith B, Smith R, Soper F, Sparrow B, Standish RJ, Staples TL, Stephens R, Szota C, Taseski G, Tasker E, Thomas F, Tissue DT, Tjoelker MG, Tng DYP, de Tombeur F, Tomlinson K, Turner NC, Veneklaas EJ, Venn S, Vesk P, Vlasveld C, Vorontsova MS, Warren CA, Warwick N, Weerasinghe LK, Wells J, Westoby M, White M, Williams NSG, Wills J, Wilson PG, Yates C, Zanne AE, Zemunik G and Ziemińska K (2021) 'AusTraits, a curated plant trait database for the Australian flora', *Scientific Data*, 8(1):254, doi:10.1038/s41597-021-01006-6.

Kotzur I, Boer M, Yebra M and Moore BD (2026) 'Monitoring Forest Foliar Moisture Using Sentinel-2 Reflectance and Radiative Transfer Model Inversion in Australia', *IEEE Journal of Selected Topics in Applied Earth Observations and Remote Sensing*1–18, doi:10.1109/JSTARS.2026.3704632.

National Bushfire Intelligence Capability (2026) 'National Bushfire Historical Extents', https://data.gov.au/data/dataset/468af92d-88c0-49ba-8738-7efd7df06727.

Roff A, Day M, Thonell J and Denholm B (2022) *NSW State Vegetation Type Map: Technical Notes*, NSW Department of Planning and Environment, Parramatta, Australia.

Su C-H, Torrance J, Rennie S, Howard E, Stassen C, Warren R, Smith A, Dharssi I, Pepler A, Tian S, Lipson M, Steinle P, Franklin C, Le T, Wang C, Masoumi S and Le Marshall J (2025) 'The Australian regional atmospheric reanalysis system, version 2 – BARRA2', *Journal of Southern Hemisphere Earth Systems Science*, 75(3):ES25032, doi:10.1071/ES25032.

Takaku J, Tadono T, Doutsu M, Ohgushi F and Kai H (2021) ‘Updated Of “AW3D30” ALOS Global Digital Surface Model In Antarctica With Other Open Access Datasets’, *The International Archives of the Photogrammetry, Remote Sensing and Spatial Information Sciences*, XLIII-B4-2021:401–408, doi:10.5194/isprs-archives-XLIII-B4-2021-401-2021.

Zanaga D, Van De Kerchove R, Daems D, De Keersmaecker W, Brockmann C, Kirches G, Wevers J, Cartus O, Santoro M, Fritz S, and others (2022) ‘ESA WorldCover 10 m 2021 v200’.